Mechanically reinforced hydrogel vehicle delivering angiogenic factor for beta cell therapy

Toftdal, Mette Steen; Christensen, Natasja Porskjær; Kadumudi, Firoz Babu; Dolatshahi-Pirouz, Alireza; Grunnet, Lars Groth; Chen, Menglin

Published in:
Journal of Colloid and Interface Science

Link to article, DOI:
10.1016/j.jcis.2024.04.050

Publication date:
2024

Document Version
Publisher's PDF, also known as Version of record

Journal of Colloid and Interface Science 667 (2024) 54–63

Contents lists available at ScienceDirect

Journal of Colloid And Interface Science

journal homepage: www.elsevier.com/locate/jcis

Regular Article

Mechanically reinforced hydrogel vehicle delivering angiogenic factor for beta cell therapy

Mette Steen Toftdal [a,b], Natasja Porskjær Christensen [a], Firoz Babu Kadumudi [c], Alireza Dolatshahi-Pirouz [c], Lars Groth Grunnet [b], Menglin Chen [a,*]

[a] Department of Biological and Chemical Engineering, Aarhus University, 8000 Aarhus C, Denmark
[b] Department of Cell Formulation and Delivery, Novo Nordisk A/S, 2760 Måløv, Denmark
[c] Department of Health Technology, Technical University of Denmark, 2800 Kongens Lyngby, Denmark

GRAPHICAL ABSTRACT

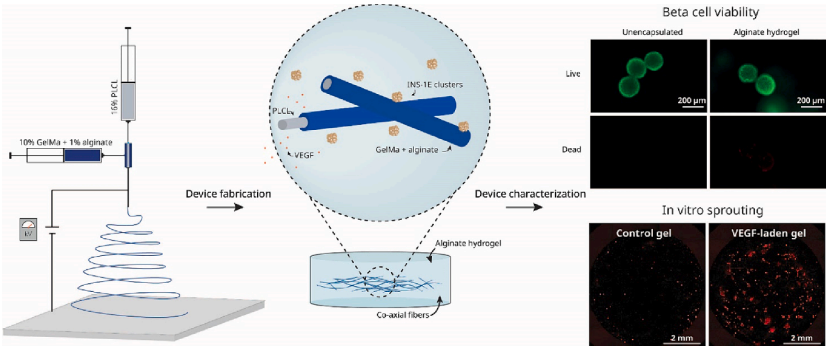

ARTICLE INFO

Keywords:
Drug release
Beta cell
VEGF
Electrospinning
Hydrogel

ABSTRACT

Type 1 diabetes mellitus (T1DM) is a chronic disease affecting millions worldwide. Insulin therapy is currently the golden standard for treating T1DM; however, it does not restore the normal glycaemic balance entirely, which increases the risk of secondary complications. Beta-cell therapy may be a possible way of curing T1DM and has already shown promising results in the clinic. However, low retention rates, poor cell survival, and limited therapeutic potential are ongoing challenges, thus increasing the need for better cell encapsulation devices. This study aimed to develop a mechanically reinforced vascular endothelial growth factor (VEGF)-delivering encapsulation device suitable for beta cell encapsulation and transplantation. Poly(l-lactide-*co*-ε-caprolactone) (PLCL)/gelatin methacryloyl (GelMA)/alginate coaxial nanofibres were produced using electrospinning and embedded in an alginate hydrogel. The encapsulation device was physically and biologically characterised and was found to be suitable for INS-1E beta cell encapsulation, vascularization, and transplantation in terms of its biocompatibility, porosity, swelling ratio and mechanical properties. Lastly, VEGF was incorporated into the hydrogel and the release kinetics and functional studies revealed a sustained release of bioactive VEGF for at

* Corresponding author.
E-mail address: menglin@bce.au.dk (M. Chen).

https://doi.org/10.1016/j.jcis.2024.04.050
Received 12 October 2023; Received in revised form 18 March 2024; Accepted 8 April 2024
Available online 9 April 2024

least 14 days, making the modified alginate system a promising candidate for improving the beta cell survival after transplantation.

1. Introduction

Type 1 diabetes mellitus (T1DM) is a chronic and potentially fatal disease, which globally affects millions of patients. It is characterised by an autoimmune destruction of the insulin-producing beta-cells leading to insulin deficiency [3,49]. Exogenously delivered insulin is currently the gold standard for treating T1DM, however, it does not completely recapitulate the normal glycaemic balance in patients. Poor glycaemic control may lead to hyperglycaemic episodes that may increase the risk of getting long-term secondary complications such as cardiovascular diseases, peripheral neuropathy, diabetic nephropathy, or retinopathy or lead to hypoglycaemic episodes which ultimately can be fatal [14;49]. Due to this, transplantation of insulin-producing cells, such as native pancreatic islets or stem cell-derived beta-like cells, has been widely investigated in recent years as a potential cure for T1DM [9,12]. More than 1,500 diabetic patients have undergone pancreatic islet transplantation with 50–70 % of the patients remaining insulin-independent after 5 years [39]. Even though numerous studies have shown promising results in regard to reaching insulin independence after islet transplantation, low retention rates, cell survival and limited therapeutic potential have been reported [52,39,48], thus resulting in an increased need for islets or beta cells per transplant.

Designing biomaterial systems that can mimic the native extracellular matrix (ECM) to ensure high cell retention and protect the therapeutic cells, may improve cell survival and ultimately enhance the efficacy of cell therapeutic tools [15,41]. Besides serving as delivery platforms which support three-dimensional (3D) beta cell encapsulation, these biomaterial systems may be engineered to exert drug delivery functions to overcome challenges such as hypoxia and foreign body response, and improve both cell survival and functionality, ultimately leading to enhanced therapeutic potential of the transplanted cells [9,12,42].

Cell delivery systems may be fabricated from numerous different biomaterials in various ways. The naturally occurring polymer, alginate, has been widely used for beta cell encapsulation, due to its quick and nontoxic gelation properties and corresponding low cytotoxicity. Alginate alone, however, has been reported to possess limited mechanical strength; hence, complicating the transplantation and retrieval procedure [13]. Therefore, alginate can ideally be mechanically reinforced to both improve the transplantation process and ensure complete graft retrieval in case needed [13,45]. Synthetic polymers, on the other hand, often have tuneable degradability, good mechanical properties, and high reproducibility [22]. Poly(ι-lactide-*co*-ε-caprolactone) (PLCL) is a biocompatible co-polymer composed of polycaprolactone (PCL) and polylactic acid (PLA) and has tailorable degradation and mechanical properties, making it ideal for mechanical reinforcement [2,31].

Electrospinning is a fibre fabrication technique often applied in tissue engineering and regenerative medicine, as it can be used to produce biocompatible scaffolds with nano-scale topography resembling the natural ECM using both naturally occurring and synthetic biomaterials [41]. Furthermore, electrospinning can straightforwardly incorporate drugs, making this fabrication method ideal as a drug delivery tool. [50,34,46]. Electrospun fibres have, furthermore, been used to mechanically reinforce hydrogels to obtain improved properties of the cell-laden systems. [12].

After the transplantation of biomaterial constructs, the therapeutic cells solely rely on oxygen diffusion for survival, as the constructs are not yet vascularized. Oxygen is diffusion limited to 100 μm and the biomaterial barrier often severely restricts the diffusion of oxygen and creates a hypoxic environment that limits the therapeutic potential of the transplanted cells [11,28,42]. As beta cells are highly sensitive to hypoxic environments due to their high metabolic activity [36,11], this is one of the key challenges to overcome in beta cell therapy. This challenge has been tackled in several ways, such as inducing vascularization through the use of growth factors, encapsulating clusters in pre-vascularized environments, or by utilizing oxygenating compounds or constructs [25,42,44,47]. The vaascular endothelial growth factor (VEGF) is well-known for its angiogenic effect and is thus widely used to improve the vascularization process *in vivo* and thereby reduce the duration of the hypoxic environment surrounding the therapeutic cells. Weaver et al. have recently shown that a VEGF-laden hydrogel system could improve islet engraftment and increase the therapeutic outcome in a mouse model as a response to local delivery of VEGF [47]. Similar findings have been reported by Yin and colleagues, who developed a VEGF-conjugated alginate encapsulation device, that improved islet engraftment and function in response to induced vascularization. [51] VEGF-A is the most extensively studied protein of the VEGF family due to its crucial involvement in wound healing and tissue repair, as VEGF-A expression is upregulated in response to hypoxia in tissues. Notably, VEGF-A exists in multiple isoforms, with VEGF-A165 being the most biologically active and prevalent variant [29]. Developing a VEGF-releasing hydrogel may improve cell viability by speeding up the vascularization process.

In this study, a biocompatible alginate hydrogel was mechanically reinforced using coaxial PLCL/GelMA/alginate nanofibres. The fibre core was composed of the mechanically robust PLCL and the fibre shell was made from the hydrophilic and biocompatible GelMa and alginate to ensure quick gelation and incorporation into the cell-laden hydrogel matrix. VEGF-A was incorporated into the hydrogel to induce vascularization and the delivery function was quantified by a VEGF release and bioactivity study. Device morphology, swelling, degradation and mechanical properties were characterised by scanning electron microscopy (SEM), material weight analysis, and compression and tensile tests, respectively. The hydrogel biocompatibility was investigated by assessing the viability and functionality of encapsulated INS-1E beta cell clusters. Our findings revealed that incorporation of coaxial nanofibres resulted in a mechanically reinforced alginate hydrogel. Moreover, the developed system displayed high beta cell survival after encapsulation. Additionally, we successfully incorporated VEGF into the system and confirmed its ability to induce endothelial cell sprouting *in vitro*.

2. Methods

2.1. Preparation of polymers

Different polymer solutions were prepared one day prior to electrospinning to allow the complete dissolution of the materials. The fibre core solution was prepared by dissolving 16 % (w/v) PLCL (70:30 lactic acid: caprolactone, Resomer, Evonic) in 1,1,1,3,3,3-Hexafluoro-2-propanol (Fisher Scientific) (HFIP). The fibre shell solution was composed of 10 % (w/v) GelMA and 1 % (w/v) sodium alginate dissolved in HFIP. GelMA was prepared in-house in advance from porcine skin gelatine (Sigma Aldrich, Germany) (**Supplementary figure S1**). Firstly, 10 % (w/v) gelatine was dissolved at 60 °C in PBS (Sigma Aldrich, Germany) and left overnight under stirring conditions. Then, 10 % (v/v) methacrylic anhydride (Sigma Aldrich, Germany) was added to the gelatine solution at a rate of 0.5 ml/min and allowed to react for 3 h at 50 °C under stirring conditions, before warm PBS was added to reach a 5X dilution. Hereafter, the GelMA solution was dialyzed at 50 °C under stirring conditions against distilled water using 14 kDa cut-off dialysis bags (Merck, Sigma Aldrich, Germany). Lastly, the GelMA solution was lyophilized.

2.2. Electrospinning

Two syringes containing the core and shell solutions were connected to a coaxial needle (inner diameter: 0.7 mm, outer diameter: 1.8 mm), placed 11 cm from the collector drum. The electrospinning process was performed at room temperature with a constant polymer flow rate of 0.5 mL/h and 15 kV. The flow rate was controlled by two independent syringe pumps (RS-232, World Precision Instruments, FL, USA).

After electrospinning, the fibre mesh was cross-linked in milli-Q water containing 2 % $CaCl_2$ and 0.1 % Igracure H2959 photoinitiator (Ciba Specialty Chemicals) for 10 min under 365 nm UV light. After cross-linking the fibres were washed in milli-Q water to remove excess cross-linking solution before they were lyophilized and kept at −20 °C until further use. Prior to any experiments, the fibres were sterilized under 254 nm UV for 30 min on each side.

2.3. Hydrogel formation

To manufacture the alginate hydrogels used for the following studies, 30 μL (unless otherwise specified) 2 % (w/v) PRONOVA SLG100 alginate (NovaMatrix, Norway) was deposited in a casting mould with the following dimensions: H:1.8 mm, Ø:4.6 mm. The alginate solution was cross-linked for 2 min by adding 30 μL 100 mM $CaCl_2$ on top, before the hydrogels were removed from the casting moulds and submerged in the 100 mM $CaCl_2$ solution to ensure full cross-linking of the entire system. Then the hydrogels were immediately transferred to buffer or media (as described according to each study) and incubated at 37 °C. The fibre-laden hydrogel was prepared by inserting an electrospun fibrous disk (diameter: 4 mm) into the alginate solution using forceps, prior to crosslinking of the system. The dry mass ratio between the fibre and the alginate of the composite system was 1:6.7. Table 1 presents an overview of the different hydrogel groups used for the experiments.

2.4. Swelling and degradation

To evaluate the physical properties of the alginate hydrogel and the coaxial fibres, swelling ratio and degradation profile were investigated. Hydrogels with a volume of 50 μL and 12 mm fibre scaffolds were used for both swelling and degradation studies. The swelling ratio was examined by immersing hydrogels and fibres in Hanks' Balanced Salt solution (Merck, Sigma Aldrich, Germany) (HBSS) supplemented with 3 mM $CaCl_2$ and incubating them at 37 °C. At every time point, the wet weight (W_w) was measured, and samples were frozen. After finalizing the experiment, the samples were lyophilized for 24 h and the dry weight was measured (W_d). The swelling ratio was calculated at 0, 2, 4, 24, 48, 72, 168, and 336 h for N = 3 using the following equation:

$$Swellingratio = \frac{W_w - W_d}{W_d} \quad (1)$$

The degradation profiles were characterised by immersing hydrogels and fibres in PBS (without Ca and Mg) and incubating them at 37 °C. At every time point, samples were frozen and after the experiment, lyophilized for 24 h before W_d was measured. Degradation was calculated at 0, 3, 8, 24, 48, 120, 192, 336, and 672 h for N = 4 using the following equation:

$$Degradation = \frac{W_d}{W_{d,0h}} \times 100 \quad (2)$$

Table 1
Overview of different hydrogel test groups.

Test groups	Explanation
No Fibre	Alginate hydrogel without fibres
With Fibre	Alginate hydrogel with fibres incorporated
Unencapsulated	Unencapsulated IN-1E clusters used as controls
Alginate hydrogel	Encapsulated INS-1E beta cell clusters encapsulated in the alginate hydrogel
VEGF-laden gel	Alginate hydrogel loaded with VEGF (no cells encapsulated)
Control gel	Alginate hydrogel with no VEGF (no cells encapsulated)

2.5. Scanning electron microscopy

The fibre morphology and hydrogel porosity were examined using scanning electron microscopy (TM3030Plus, HITACHI, Japan) (SEM). The SEM was operated with an acceleration voltage of 15 kV and both backscattered and secondary electrons were used for imaging. The morphology was obtained using ImageJ software by measuring fibre diameter or pore size on each image (N = 3).

2.6. Mechanical studies

The mechanical tensile and compression behaviour of pure alginate hydrogels and fibre-reinforced hydrogels were characterised using an Instron mechanical tester (model 5967, U.K). Hydrogels were prepared according to **section 2.3**, one day in advance of the mechanical test and incubated in RPMI 1640 (Gibco, Thermofisher, MA, USA) media at 37 °C. For the compression tests, a constant compression rate of 0.5 mm/min was applied and the tests were performed using a 50 N load cell for N = 13. To conduct the tensile testing, 150 μL alginate solution was transferred to a mould (dimensions: L:30, H;1, W:5 mm) to create hydrogels suitable for the testing. Fibres were cut using a scalpel to obtain fibre sheets that fitted inside the hydrogels. To understand the mechanical properties of the electrospun nanofibres, pure nanofibres were likewise subjected to tensile testing. The thickness and weight were measured for each sample prior to the test. The tests were performed using a 50 N load cell and a constant tensile speed of 1 mm/min. For the pure fibres, the speed was set to 10 mm/min. For all three conditions (N = 5–6) a gauge length of 10 mm was applied. Young's modulus, toughness, breakage strain and ultimate stress were calculated from the obtained stress–strain curves. The compression modulus was calculated as the slope from 15-25 % strain and the tensile modulus was calculated as the slope from the elastic region. The toughness was calculated as the area under the curve, whereas the strain breakage was determined as the maximum strain at the breakage point and the ultimate stress as the maximum stress before breakage.

2.7. VEGF studies

2.7.1. VEGF release

Hydrogels of 50 μL containing 100 ng VEGF were submerged in 1 mL 0.1 % bovine serum albumin (BSA)/PBS to assess the release kinetics. At each time point, 150 μL PBS solution was transferred to −20 °C and replaced with 150 μL fresh 0.1 %BSA/PBS to keep the buffer volume constant at 1 mL. Time points were selected to be 3 h, 5 h, 8 h, 24 h, 48 h, 7d, 14d, 21d, and 35d. Prior to the start of the experiment, two gels were dissolved using alginate lyase (A1603-100MG, Sigma Aldrich), to quantify the initial amount of VEGF present in the hydrogel. The alginate lyase was diluted in PBS/BSA (0.1 % w/v) to reach 0.05 % (w/v) and the gel was emerged and incubated at room temperature for 30 min or until the gel was completely dissolved. VEGF was quantified by VEGF165 ELISA kit (Human) (OKCDO4194-96, BioSite). The ELISA was carried out according to standard manufacturing protocol.

The accumulated VEGF release (Q) was calculated according to the following equation:

$$Release = \frac{V^*C_n + V_s^*\sum_{i=1}^{n-1} C_i}{m} * 100\% \quad (3)$$

Where V is the reaction volume, V_s is the sampling volume, C_n is the concentration in the sample well at the timepoint n, and C_i is the concentration at previous time points.

2.7.2. HUVEC sprouting and VEGF bioactivity

Human umbilical vein endothelial cells (HUVECs) were cultured in coculture with human induced pluripotent stem cells derived mesenchymal stromal cells (hIPSC-MSCs) to assess the effect of VEGF. EGM Endothelial Cell Growth Medium BulletKit (Lonza) was used to maintain the HUVECs and low glucose DMEM (Merck, Sigma Aldrich, Germany) supplemented with 10 % FBS 100 U/mL penicillin, and 100 μg/mL streptomycin was used for hIPSC-MSC maintenance. HUVECs were used between p6-p9 and hIPSC-MSC were used between p8-p10.

To evaluate the bioactivity of the released VEGF, HUVEC sprouting was first evaluated in response to VEGF to find the optimum concentration for sprouting. HUVECs and hIPSC-MSCs were harvested and seeded in a 96-well plate at a ratio of 1:4 (3,000 HUVEC:12,000 hIPSC-MSC per well) in EGM growth medium. 24 h after seeding, 0–60 ng/mL rhVEGF 165 (R&D systems, MN, USA) or medium from VEGF-releasing hydrogel cultures were added to the medium. The cells were cultured at 37 °C, 5 % CO_2, and 90 % humidity and the medium was replaced every 2–4 days.

After 9–11 days of culture, the cells fixed using 4 % paraformaldehyde (Sigma Aldrich, Germany). To prevent unspecific antibody binding, the cells were blocked with 1 % BSA in PBS for 45 min before they were rinsed with PBS. 5 μg/mL anti-CD31, rabbit polyclonal antibody (abcam, ab32457, UK) in 1 % BSA/PBS was added to the wells and left at 4 °C overnight. The cells were rinsed with PBS prior to staining with 1:1000 Anti-rabbit 594 IgG (abcam, ab150076, UK) in 1 % BSA/PBS for 1 h at room temperature. Lastly, the cells were rinsed with PBS and stained with Hoechst 33,342 (Invitrogen, ThermoFischer, MA, USA) for 10 min and imaged using EVOS™ M7000 Imaging System (Invitrogen, ThermoFischer, MA, USA). The CD31 stained area of the entire well was quantified using ImageJ software (N = 3).

2.8. Beta cell culture, cluster formation and encapsulation

To investigate cell viability and performance in an encapsulated environment, INS-1E reporter cells were encapsulated in the alginate hydrogels. The INS-1E reporter cell line (hereafter called INS-1E cells) is derived from genetically modifying the INS-1E rat insulinoma cell line [23,35] to co-secrete luciferase in a 1:1 ratio with insulin as described by [8] and was used for all beta cell experiments.

The INS-1E cells were cultured in growth medium containing RPMI 1640 (Gibco, Thermofisher, MA, USA), 10 % heat-inactivated Fetal Bovine Serum (FBS) (Gibco, Thermofisher, MA, USA), 100 U/mL penicillin (Gibco, Thermofisher, MA, USA), 100 μg/mL streptomycin (Gibco, Thermofisher, MA, USA), and 50 μM 2-mercaptoethanol (Gibco, Thermofisher, MA, USA).

To mimic the nature of pancreatic islets, INS-1E clusters were formed from single cells. The clusters were formed by transferring 7.5×10^6 cells in 10 mL growth medium containing 10 μM Rock-Inhibitor (Roche) and 50 μg/mL DNase (Sigma Aldrich, Germany) to a non-adherent 10 cm petri dish. The cells were cultured at 70 RPM for two days to obtain ≈ 1000 islet equivalent (IEQ)/mL. INS-1E cell clusters were counted (Automatic Islet Cell Counter, Biorep Technologies, FL, USA) and encapsulated in alginate. Clusters were encapsulated with a density of 10,000 IEQ/mL and mixed with alginate before the hydrogels were cross-linked according to **section 2.3**.

2.9. Cell viability

To evaluate the cell viability up to 7 days after encapsulation in alginate hydrogels (without fibres), the encapsulated clusters were either stained with live/dead staining or subjected to the colourimetric metabolic assay Cell Counting kit-8 (CCK8) (Dojindo, Japan). CCK8 was conducted on unencapsulated and encapsulated cells according to the manufacturer's protocol. An incubation time of 3 h was used for the study and the absorbance was measured using Varioskan LUX Multimode Microplate Reader (ThermoFisher, MA, USA). For live/dead staining, cell-laden hydrogels and unencapsulated cells were stained with 2 μM Calcein-AM (Invitrogen, MA, USA), 2 μM ethidium homodimer-1 (Invitrogen, MA, USA) and 2 μM Hoechst 33,342 (Fisher Scientific, MA, USA) in RPMI 1640. After incubation for 1 h, the staining solution was replaced with RPMI 1640, and the cells were imaged using an Olympus IX81 Inverted Fluorescence microscope (Olympus, Japan).

2.10. Cluster functionality

Cluster functionality was assessed using glucose-stimulated insulin secretion (GSIS) assay. GSIS was conducted on encapsulated INS-1E clusters to confirm their functionality after encapsulation.

One day after encapsulation, encapsulated and unencapsulated INS-1E clusters were transferred to a 96-well insert plate (40 μm filter plate, Merck, NJ, USA). Prior to the GSIS test, clusters were washed twice with Krebs Ringer Buffer with HEPES (KRBH, VWR, PA, USA) supplemented with 0.2 % (w/v) human serum albumin (Sigma Aldrich, Germany), 2 mM glutaMAX (Gibco, Thermofisher, MA, USA) (referred to as KRBH solution), and 2 mM glucose (Sigma Aldrich, Germany). The KRBH buffer contains 119 mM NaCl, 4.7 mM KCl, 2.5 mM CaCl2, 1.2 mM MgSO4, 1.2 mM KH2PO4, and 20 mM HEPES. After the washing steps, all clusters were exposed to a low glucose solution (KRBH solution supplemented with 2 mM glucose) for 1 h prior to treatment with a high glucose solution (KRBH solution supplemented with 20 mM glucose) for another hour. Then, clusters were collected in 2 mL lysis buffer containing 1 M ammonium hydroxide (Acros Organics, Fisher Scientific, Belgium) and 0.2 % (v/v) Triton X-100 (Sigma Aldrich, Germany) and stored at −20 °C before they were lysed using sonication and used for DNA quantification. The GSIS was conducted with N = 6 replicates. The supernatants from the two treatments were assayed for their luciferase content which was quantified using Nano-Glo Luciferase Assay (Promega, WI, USA) by following the manufacturer's guidelines. Samples were incubated for 10 min before they were analyzed for their luminescence intensity using a Varioskan LUX Multimode Microplate Reader (ThermoFisher, MA, USA).

The DNA content was quantified to normalize the luciferase secretion obtained from the GSIS assay. DNA quantification was conducted using the fluorescence-based Quant-iT PicoGreen dsDNA assay kit (Invitrogen Thermofisher, MA, USA) by following the manufacturer's guidelines. The DNA standard was used to prepare a standard curve ranging from 1 to 600 ng DNA/mL. All samples were incubated at room temperature without light for 3 min, prior to measuring sample fluorescence using the Varioskan LUX Multimode Microplate Reader (excitation 485 nm, emission 525 nm).

3. Results and discussion

3.1. Hydrogel and fibre fabrication

In order to manufacture the fibre-reinforced hydrogel, PLCL/GelMA/Alginate nanofibres were electrospun using a coaxial needle (Fig. 1**A**) to obtain hydrophilic fibres in a convenient one-step manner. The hydrophilic shell played a crucial role in facilitating the integration of fibres into the alginate hydrogel.

The fibres with an average diameter of 892.7 ± 164.8 nm were found to be homogeneously distributed in the fibre patch and a bead-free morphology was observed (Fig. 1**B and C**), which correlates with what has previously been reported [2]. Hydrogel porosity is crucial in supporting both cell survival and functionality upon encapsulation. The pores were found to be interconnected (Fig. 1**D**), which is vital for allowing sufficient fluid exchange and ensuring the transport of nutrients, oxygen, insulin, and waste products. The average pore diameter (Fig. 1**E**) was found to be 178 ± 95 μm, which is within the optimal pore size range of 50 to 300 μm for inducing vascularization inside the hydrogel [10,16]. It is noted that pore size measurement based on SEM imaging after lyophilization is not accurate, since the lyophilization

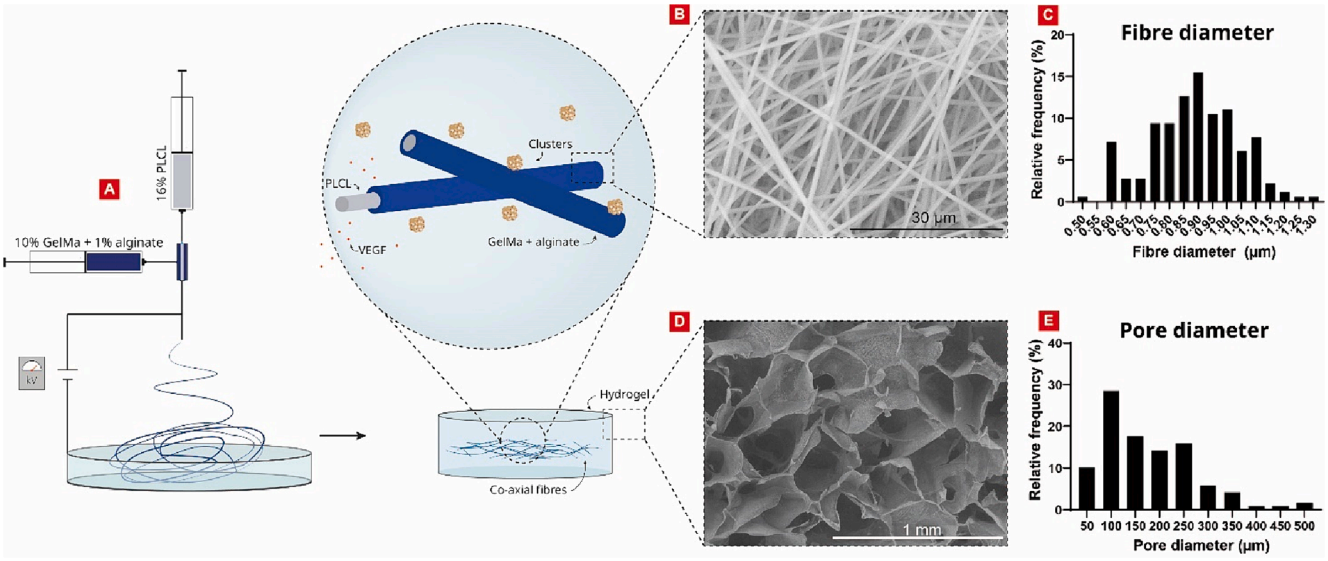

Fig. 1. Hydrogel and fibre fabrication and characterisation. A) The electrospinning set-up used to manufacture coaxial nanofibres. The nanofibres were embedded in alginate hydrogels encapsulating beta cell clusters. VEGF was incorporated into the device for delivery. B) SEM image of the coaxial fibres, where the fibre diameter C) was quantified. D) SEM image of the porosity of a lyophilized hydrogel. E) Pore diameter quantified from the hydrogel SEM image.

process, such as freezing rate, influences the pore size after ice crystals sublimation.

3.2. Physical and mechanical characterisation

The fibrous alginate hydrogel system was physically and mechanically characterised to investigate its suitability for beta cell therapy in terms of encapsulation and transplantation.

The mechanical properties of alginate alone have previously been reported to be inadequate for transplantation purposes [12]. To achieve mechanical robustness, we reinforced the hydrogels with mechanically robust PLCL/GelMa/Alginate core–shell nanofibers (**Supplementary Figure S2**). Mechanical tensile tests were conducted to compare the fibrous hydrogels with pure alginate hydrogels (Fig. 2**A and Supplementary Figure S3**). The Young's modulus was found to be significantly improved by the addition of the nanofibres from 6.3 ± 0.8 kPa to 73.5 ± 24.6 kPa, making the system more elastic and capable of withstanding tensile stress. Furthermore, the nanofibres were found to increase the

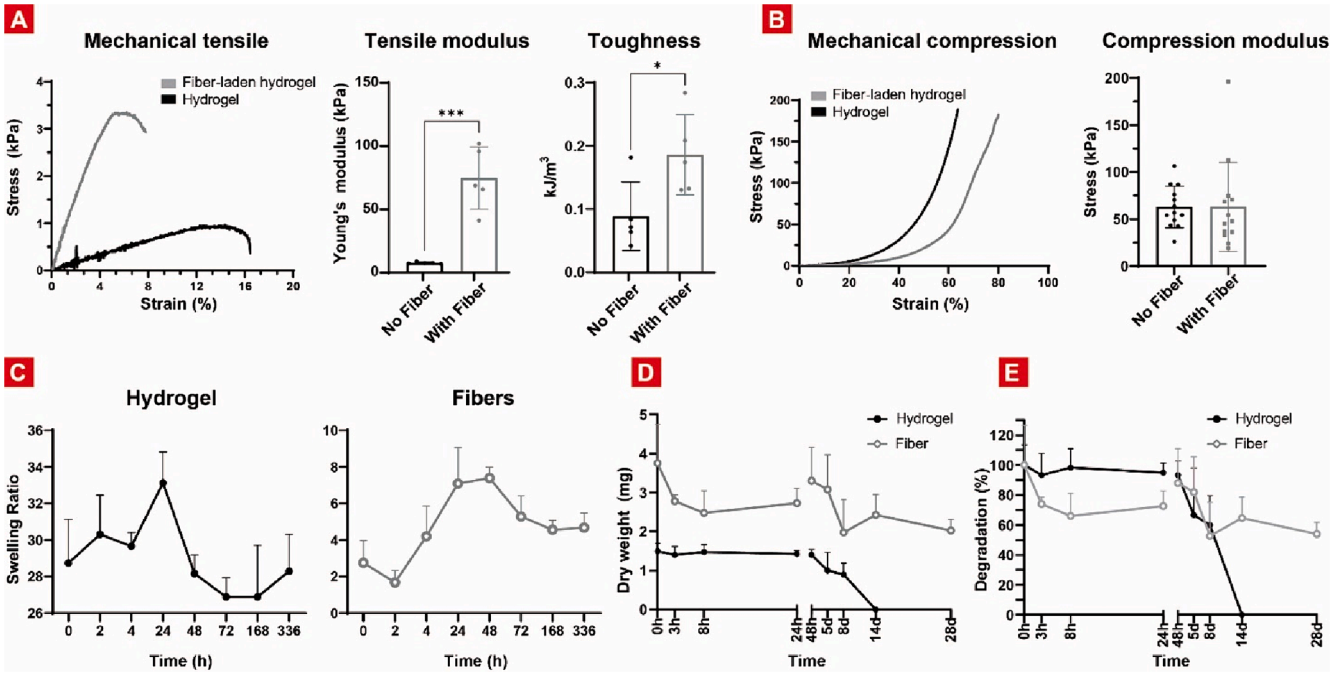

Fig. 2. Physical and mechanical device characterisation of hydrogels with and without embedment of fibres. A) Stress–strain curve obtained by mechanical tensile testing and the calculated tensile modulus and toughness for n = 5 replicates. B) Stress–strain curve obtained by the mechanical compression test and the coherent compression modulus. The compressions were run until 80 % strain for n = 13 replicates. C) The calculated swelling ratio monitored for 14 days for both alginate hydrogels and PLCL/GelMA/Alg coaxial fibres for n = 3 replicates. D) Dry weight of the fibre and hydrogel monitored for 28 days and E) the corresponding degradation profile for n = 4 replicates. Data is presented as the mean ± standard deviation, where the individual dots in the mechanical tests represent sample replicates.

toughness of the hydrogel from 0.09 ± 0.05 kJ/m^3 to 0.16 ± 0.08 kJ/m^3 which makes the hydrogel more resistant to fracture when stressed. These observations confirm that the incorporation of nanofibres significantly improved the mechanical properties of the encapsulation system, creating a device that is more likely to be successfully transplanted and retrieved without breakage in case of any health concerns. Like Young's modulus and toughness, the ultimate stress was found to be significantly improved from 1.0 ± 0.3 kPa to 3.3 ± 1.5 kPa by the addition of the nanofibres, whereas the strain breakage significantly decreased from 15.8 ± 4.4 % to 7.4 ± 1.9 % (**Supplementary Figure S3**). Besides tensile testing, the fibre-laden hydrogels were compared to hydrogels without fibres in terms of mechanical compression (Fig. 2**B and Supplementary Figure S4**) to ensure that the compression properties were compatible with the transplantation sites. [17]. The compressive modulus of the fibre-laden hydrogel and the pure hydrogel was found to be 63.1 ± 47.3 kPa and 62.8 ± 22.0 kPa, respectively. Pancreatic islets or beta-cell clusters have been transplanted in rodents to a wide range of sites such as intrahepatic sites, intraperitoneal space, kidney capsules, and the subcutaneous space to find the optimal transplantation site for clinical purposes. [4,24,12,27,37]. Most of these tissues have an elastic modulus of approximately 10–100 kPa [17], making the compressive modulus of both the fibre-laden and pure hydrogel ideal for beta-cell transplantations. Like the compressive modulus, toughness, strain breakage, and ultimate stress were not significantly affected by the incorporation of the nanofibres (**Supplementary Figure S4**).

The native tissue is highly hydrated which makes the hydration of a biomaterial system a critical factor to investigate to ensure high cell viability [19]. Thus, the swelling ratio of both the alginate hydrogel and PLCL/GelMa/Alginate nanofibres were investigated (Fig. 2**D**). The swelling ratio of the alginate hydrogel was found to reach its maximum swelling ratio of 34.1 ± 1.7 after 24 h before it decreased and remained stable around 27 (Fig. 2**D**). This observation correlates with other alginate systems [19] and is within the range of biocompatible commercially available hydrogel systems such as HyStem and Glycosil. The maximum swelling ratio of the fibres, on the other hand, was found to be 7.4 ± 0.6 after 48 h, before it decreased and remained stable at around 4.5 (Fig. 2**D**). The swelling ratio of the fibres was, as expected, found to be lower compared to the hydrogel, due to the hydrophobic PLCL comprising 60 % of the total fibre mass.

Hydrogel and fibre degradation were investigated as polymer weight loss as a function of time in a 28-day study. Both device components were incubated separately in PBS (without calcium and magnesium) and the dry weight was monitored at specific time points (Fig. 2**E**). The hydrogels remained stable for 48 h before starting to degrade (Fig. 2**F**). After 14 days, all hydrogels were completely degraded. The coaxial fibres, on the other hand, were slowly degraded during the entire experiment, however, 60 % of the fibre weight remained after 28 days of incubation. Complete degradation of PLCL (PLCL 70:30) due to hydrolysis has been reported to last up to a year [18], thus indicating that the 40 % fibre weight loss most likely was due to GelMA/Alginate shell degradation, which corresponds to 40 % of the total fibre mass. The hydrogel and fibre degradation will be discussed further in the VEGF release section.

3.3. *Alginate biocompatibility*

To confirm high biocompatibility of alginate, cell viability and functionality were investigated for clusters encapsulated in pure alginate. From the live/dead stain on day 1(Fig. 3**A**), it was evident that the cluster viability of the encapsulated clusters was high, and that alginate was fully comparable to the unencapsulated culture condition. This observation was further confirmed by CCK-8 viability measurements up to day 3 (Fig. 3**B**), which likewise showed viable and proliferating cells comparable to unencapsulated clusters, verifying great beta-cell compatibility of the hydrogel. The metabolic activity of the encapsulated clusters was found to increase for the entire experiment, showing viable cells for at least 7 days. On days 5 and 7, however, the encapsulated clusters were found to be less metabolically active compared to unencapsulated clusters. This may be explained by the cell proliferation being physically restricted compared to unencapsulated cells or by the lack of oxygen in the centre of the hydrogel [11,42]slowing down the metabolic activity, or simply affecting the viability of the clusters in the middle of the hydrogel. When developing a beta-cell encapsulation device, it is essential that the cells not only survive but also remain

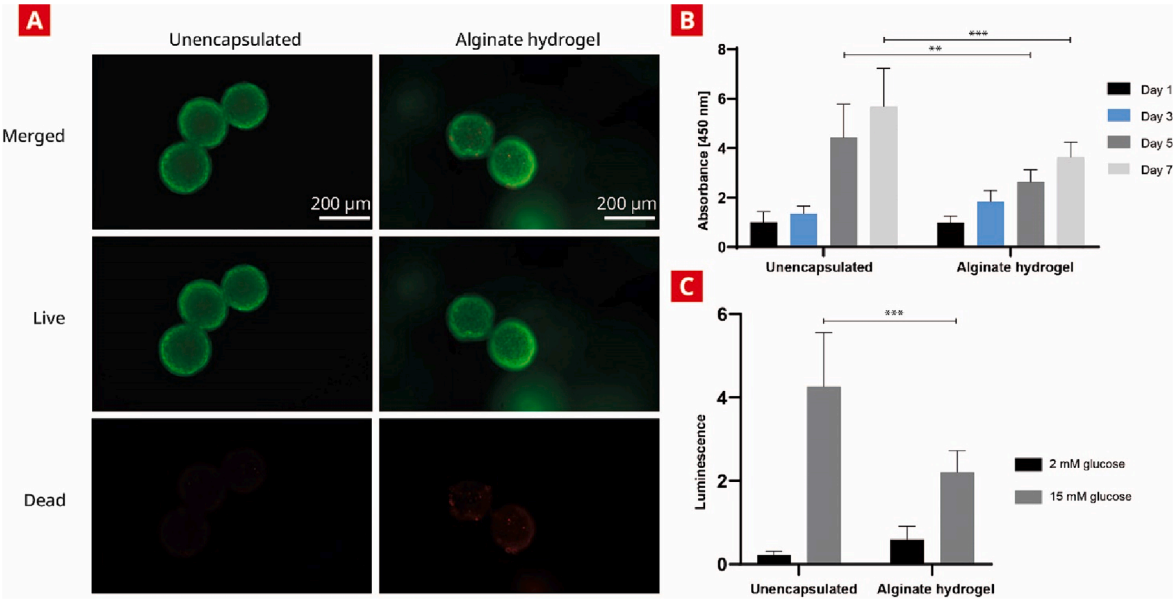

Fig. 3. Cell viability and functionality of alginate encapsulated INS-1E clusters. A) Live/dead stain of encapsulated and unencapsulated clusters on day 1 for n = 4 replicates. The green colour represents living cells, and the red colour represents dead cells. B) CKK-8 measurements of unencapsulated clusters and clusters encapsulated in alginate. Data is normalized to day 1 for n = 6 replicates. C) Functionality testing using GSIS comparing unencapsulated and encapsulated clusters on day 1. The black columns represent the first stimuli with low glucose solution and the grey columns represent the second stimuli using high glucose. Data is normalized to the DNA content for n = 6 replicates. Data is presented as the mean ± standard deviation. (For interpretation of the references to colour in this figure legend, the reader is referred to the web version of this article.)

functional after encapsulation. To assess this, unencapsulated and encapsulated INS-1E clusters were exposed to high and low glucose concentrations in a GSIS test. As the INS-1E cells secrete luciferase in a 1:1 ratio with insulin [8], luciferase was quantified and used as a measure of functionality.

Fig. 3**C** illustrates the luciferase secretion as a surrogate of insulin secretion in response to glucose stimulation. As expected, the luciferase secretion was low, when cells were stimulated with low glucose, before it increased significantly after exposing the cells to a high glucose concentration for 1 h. Cells encapsulated in alginate for 1 day, however, secreted significantly less luciferase compared to the unencapsulated cells during stimulation with high glucose. As great cluster viability was confirmed in alginate hydrogels on day 1, it could indicate that the hampered luciferase secretion was a consequence of diffusion limitations of glucose and luciferase enzyme. Hampered functionality due to encapsulation has previously been reported for clusters of encapsulated hydrogels. [7] The diameter of the encapsulation device has been found to greatly affect the total amount of released insulin. Larger devices (>1800 μm) have been found to secrete less insulin compared to smaller devices (<700 μm) and unencapsulated cells.[7] The diameter of the alginate device was 4550 μm, which therefore could explain the decreased luciferase secretion of alginate-encapsulated clusters compared to unencapsulated clusters. A way to overcome this issue could be to redesign the hydrogel shape and decrease the diameter to improve the diffusion limitation. An example of this can be found by Ernst *et al.*, who developed a toroidal-shaped hydrogel, which was found

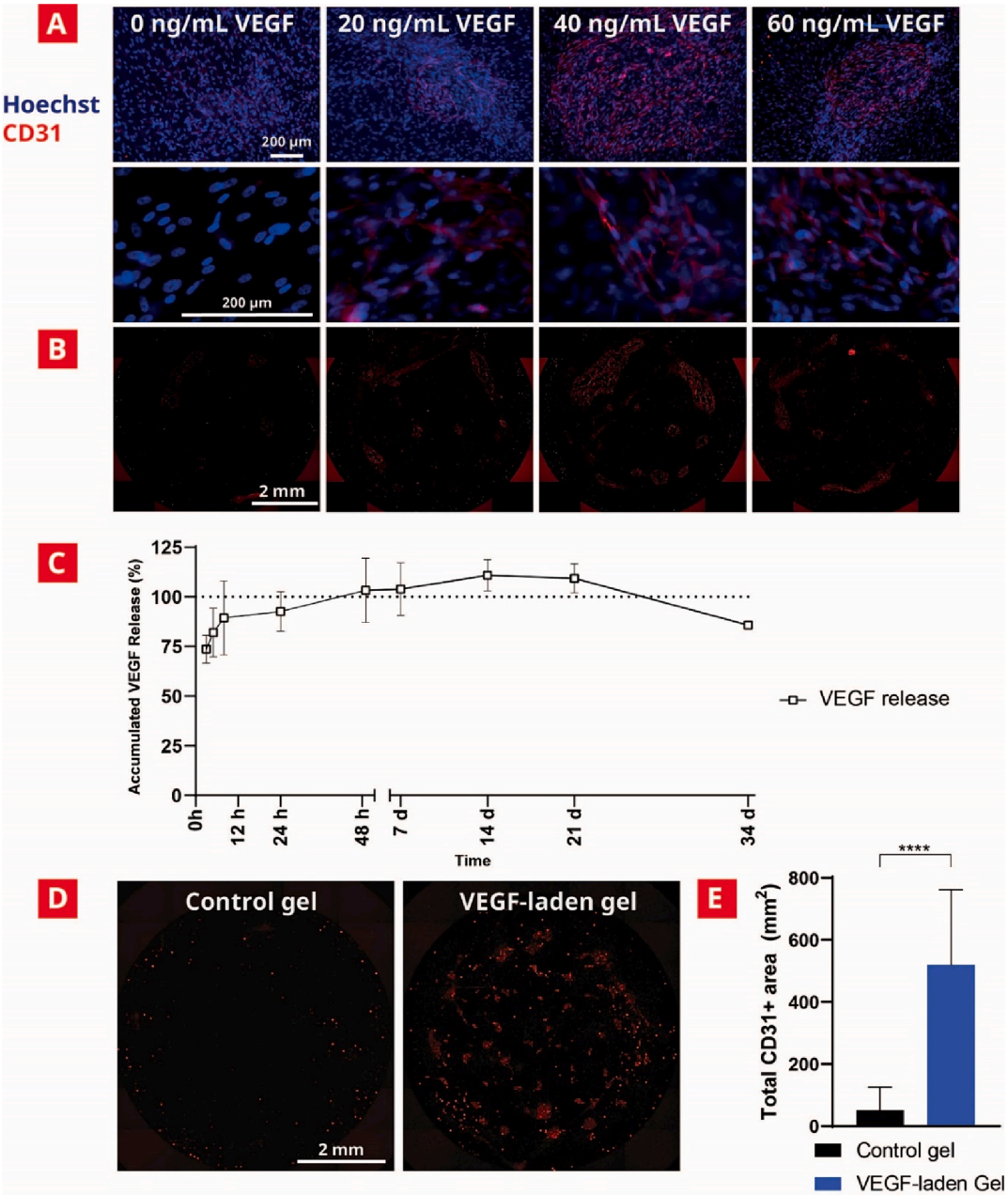

Fig. 4. VEGF incorporation, release and function. A) VEGF dose–response study conducted in HUVEC and iPSC-derived MSC cocultures. The blue staining represents Hoechst nuclei staining, whereas the red stain represents CD31 positive cells. B) CD31 positive cells on a stitched image showing the entire culture well for n = 2C) Release kinetics of VEGF for n = 3 replicates. D) CD31 positive cells on a stitched image showing the entire culture well. HUVEC and iPSC-derived MSC were cocultured in media from gels with or without VEGF. E) The total CD31 positive area of the images in D) for n = 7 replicates. Data is presented as the mean ± standard deviation. (For interpretation of the references to colour in this figure legend, the reader is referred to the web version of this article.)

to improve diffusion throughout the entire device. [12] Another approach to overcome the diffusion barrier could be to increase the porosity of alginate. Lui and co-workers developed a porous alginate encapsulation capsule using polyethene oxide as a pore-making agent and reported that the insulin secretion from encapsulated beta cells was comparable to the one of unencapsulated beta cells. [32]

3.4. VEGF release and sprouting

The angiogenic growth factor VEGF was incorporated into the hydrogel to induce vascularization and thereby improve cell survival upon transplantation. Firstly, a VEGF dose–response study was conducted to confirm that the HUVECs were an appropriate model for assessing VEGF bioactivity and finding the optimum VEGF concentration to stimulate *in vitro* sprouting (Fig. 4**A and B**). Then, to explore the incorporation of the protein into the alginate hydrogel and assess the VEGF release kinetics, a release study was conducted (Fig. 4**C**). Lastly, the bioactivity of the released VEGF (Fig. 4**D and E**) was investigated to confirm its biological effect on endothelial cells.

It is well known that MSCs induce HUVEC sprouting by supporting endothelial cell tubular network formation. The full mechanism of this process is not yet completely understood; however, MSCs are thought to secrete growth factors such as VEGF and other cytokines to stimulate the angiogenic process [53,5]. Because of this, HUEVCs were cocultured with hIPS-MSC in growth media containing 0–60 ng VEGF/mL and stained for the endothelial cell marker CD31, to find the optimum concentration for sprouting (Fig. 4**A and B**). The HUVECs were found to change morphology and create CD31-positive cell clusters with tubular networks when increasing the concentrations of VEGF. No CD31-positive cell clusters were found in the cells cultured without VEGF, whereas these clusters were pronounced in all conditions in the presence of VEGF. A VEGF concentration of 40 ng/mL was found to give rise to the largest HUVEC clusters. This is in accordance with what has previously been reported for VEGF-stimulated sprouting by HUVECS [1]. Thus, 40 ng/mL VEGF was the aim for the VEGF release study and 100 ng VEGF was incorporated into each scaffold.

From the release study (Fig. 4**C**), a burst release was observed within the first 8 h where approximately 75 % of the total VEGF amount was released. After 14 days the accumulated VEGF release reached its maximum with approximately 100 % of the total incorporated VEGF being released. The subsequent observed decline was most likely attributed to the degradation of VEGF degradation during the incubation period, as VEGF is known to degrade at physiological temperatures with a half-life of 96 min in acellular solutions [43]. The VEGF release from the hydrogel follows a diffusion-based process, which relies on the hydrogel properties, especially its porosity. A burst release of VEGF was, therefore, expected, as the hydrogel pores were found to be interconnected with an average pore size of approximately 180 μm and VEGF is 23 kDa (homodimer form is 46 kDa). [20] It has previously been reported that an initial burst release of VEGF with high concentrations, followed by a decreasing concentration over a 4-week period yields optimal sprouting conditions. [40,38] Though the release curve exhibits an initial burst release followed by a gradual release for 14 days, the release kinetics could be further improved. As electrospun fibres are known for their excellent drug delivery properties [26,33,50], one approach to enhance the sustained release could be to incorporate VEGF into the fibres in addition to the hydrogel. This modification could potentially extend the duration of the release and thus improve the overall control of the VEGF delivery.

Compared to the degradation study, where the gels were degraded after 14 days, the gels in the release study were still intact after 34 days. This was most likely due to the presence of calcium ions in the culture media [54]. Calcium ions ensure hydrogel crosslinking and presumably stabilise the system. To test this, a degradation study was carried out in a buffer supplemented with 3 mM $CaCl_2$. After a period of 14 days, the gels remained intact, with no observed degradation in either their dry weight or morphology (**Supplementary Figure S5**). The mass of the fibres, however, increased over time, which might be explained by the buffer salts accumulating and adding to the dry weight after lyophilization. The morphology of the fibres remained mostly unaffected by the one-month incubation, similar to the observed morphological behaviour of the hydrogel (**Supplementary Figure S5**).

To confirm bioactivity, HUVEC cocultures were treated with supernatant from cultured hydrogels loaded with VEGF, control hydrogels without VEGF and pure media containing 40 ng/mL VEGF (Fig. 4**D and Supplementary Figure S6**). A similar sprouting pattern was observed in both conditions treated with supernatant from VEGF-laden hydrogels and VEGF-supplemented media, indicating that the released VEGF was indeed bioactive and was not affected by the incorporation into the hydrogel. No sprouting was observed in the control hydrogel condition. (Fig. 4**D and E**) The HUVEC cluster area in the bioactivity study (Fig. 4**D**) was observed to be smaller in comparison to the dose–response study (Fig. 4**B**). This can most likely be attributed to the degradation of VEGF at 37 degrees. In the dose–response study, VEGF-supplemented media was kept at 4 degrees, whereas the VEGF-supplemented media control in the bioactivity study was incubated at 37 degrees to ensure comparable treatment across all samples and controls.

4. Conclusion and perspectives

Beta cell delivery has shown promising results for treating type 1 diabetes. However, significant graft loss has been observed post-transplantation due to challenges such as hypoxia and lack of vascularization. [11,47] To overcome this challenge, we developed a vascular endothelial growth factor (VEGF)-releasing fibre-reinforced alginate encapsulation device. Due to alginate's weak mechanical properties [12], electrospun coaxial fibres were incorporated into the hydrogel to yield a mechanically reinforced system. The Young's modulus was improved by more than 10-fold and the toughness by almost 2-fold by the addition of fibres, creating a mechanically reinforced encapsulation device. The average pore size of the hydrogel was found to be approximately 180 μm, which is within the optimal range for inducing vascularization inside the device. The alginate hydrogel system was, furthermore, found to maintain great viability of encapsulated beta cells. In addition, the encapsulated beta cells were functional and responded to changes in glucose concentrations; however, this functionality was observed to be diminished when compared to unencapsulated clusters. Investigating whether this reduction in functionality has a physiological impact *in vivo* is crucial. Nevertheless, it underscores the significance of enhancing the diffusion properties of the hydrogel to achieve optimal therapeutic outcomes with minimal cell usage. Lastly, 100 % of the incorporated and biologically active VEGF was observed to be released during a two-week period, making the alginate system a promising candidate for improving cell survival at the transplantation site by inducing the vascularization process while simultaneously providing a biocompatible delivery vehicle for beta cells. The *in vivo* effect of the VEGF-laden device will be the next focus to be investigated to fully confirm the physiological relevance of the developed device.

One of the complex challenges of developing a clinically suitable implant is the increased immune response associated with well-vascularized implants. This study focused on ensuring cell vascularization to maintain cell functionality, a critical first step towards a therapeutically relevant device. Future work will aim to mitigate cellular overgrowth and foreign body responses by e.g. using hypoimmunogenic stealth beta cells in combination with modified alginate, which have shown promise in reducing these issues [30,6,21]. Chemically modified alginate, in particular, has been found to lessen inflammatory responses and improve the viability and function of encapsulated cells, offering a pathway to enhance the therapeutic outcome of such devices. [30]

CRediT authorship contribution statement

Mette Steen Toftdal: Conceptualization, Data curation, Investigation, Writing – original draft. **Natasja Porskjær Christensen:** Investigation, Visualization. **Firoz Babu Kadumudi:** Investigation, Methodology. **Alireza Dolatshahi-Pirouz:** Methodology. **Lars Groth Grunnet:** Conceptualization, Supervision, Writing – review & editing, Project administration. **Menglin Chen:** Conceptualization, Supervision, Writing – review & editing.

Declaration of competing interest

The authors declare that they have no known competing financial interests or personal relationships that could have appeared to influence the work reported in this paper.

Data availability

Data will be made available on request.

Acknowledgement

We gratefully acknowledge the support of Innovation Fund Denmark (9065-0021). The authors would furthermore like to thank Thomas Frogne, Department of Cell Engineering Novo Nordisk A/S for engineering the INS-1E beta cell line and Marianne Vollmond for technical assistance.

Appendix A. Supplementary data

Supplementary data to this article can be found online at https://doi.org/10.1016/j.jcis.2024.04.050.

References

[1] T. Ahlfeld, F.P. Schuster, Y. Förster, M. Quade, A.R. Akkineni, C. Rentsch, S. Rammelt, M. Gelinsky, A. Lode, 3D plotted biphasic bone scaffolds for growth factor delivery: biological Characterization in vitro and in vivo, Advanced Healthcare Materials 8 (7) (2019), https://doi.org/10.1002/ADHM.201801512.

[2] J. Amagat Molas, M. Chen, Injectable PLCL/gelatin core-shell nanofibers support noninvasive 3D delivery of stem cells, International Journal of Pharmaceutics 568 (2019) 118566, https://doi.org/10.1016/J.IJPHARM.2019.118566.

[3] American Diabetes Association. (2021). 2. Classification and Diagnosis of Diabetes: Standards of Medical Care in Diabetes—2021. *Diabetes Care*, *44*(Supplement_1), S15–S33. doi: 10.2337/DC21-S002.

[4] D. An, A. Chiu, J.A. Flanders, W. Song, D. Shou, Y.C. Lu, L.G. Grunnet, L. Winkel, C. Ingvorsen, N.S. Christophersen, J.J. Fels, F.W. Sand, Y. Ji, L. Qi, Y. Pardo, D. Luo, M. Silberstein, J. Fan, M. Ma, Designing a retrievable and scalable cell encapsulation device for potential treatment of type 1 diabetes, Proceedings of the National Academy of Sciences of the United States of America 115 (2) (2018) E263–E272, https://doi.org/10.1073/PNAS.1708806115.

[5] I. Beloglazova, V. Stepanova, E. Zubkova, K. Dergilev, N. Koptelova, P.A. Tyurin-Kuzmin, D. Dyikanov, O. Plekhanova, D.B. Cines, A.P. Mazar, Y. Parfyonova, Mesenchymal stromal cells enhance self-assembly of a HUVEC tubular network through uPA-uPAR/VEGFR2/integrin/NOTCH crosstalk. biochimica et biophysica acta (BBA) - Molecular, Cell Research 1869 (1) (2022) 119157, https://doi.org/10.1016/j.bbamcr.2021.119157.

[6] T.M. Brusko, H.A. Russ, C.L. Stabler, Strategies for durable β cell replacement in type 1 diabetes, Science 373 (6554) (2021) 516–522, https://doi.org/10.1126/science.abh1657.

[7] P. Buchwald, A. Tamayo-Garcia, V. Manzoli, A.A. Tomei, C.L. Stabler, Glucose-stimulated insulin release: Parallel perifusion studies of free and hydrogel encapsulated human pancreatic islets, Biotechnology and Bioengineering 115 (1) (2018) 232–245, https://doi.org/10.1002/BIT.26442.

[8] S.M. Burns, A. Vetere, D. Walpita, V. Dančík, C. Khodier, J. Perez, P.A. Clemons, B. K. Wagner, D. Altshuler, High-throughput luminescent reporter of insulin secretion for discovering regulators of Pancreatic Beta-cell function, Cell Metabolism 21 (1) (2015) 126–137, https://doi.org/10.1016/J.CMET.2014.12.010.

[9] G.S. Chendke, G. Faleo, C. Juang, A.V. Parent, D.A. Bernards, M. Hebrok, Q. Tang, T.A. Desai, Supporting survival of transplanted stem-cell-derived insulin-producing cells in an encapsulation Device augmented with controlled release of amino acids. *advanced*, Biosystems 3 (9) (2019), https://doi.org/10.1002/ADBI.201900086.

[10] Y.C. Chiu, M.H. Cheng, H. Engel, S.W. Kao, J.C. Larson, S. Gupta, E.M. Brey, The role of pore size on vascularization and tissue remodeling in PEG hydrogels, Biomaterials 32 (26) (2011) 6045–6051, https://doi.org/10.1016/J.BIOMATERIALS.2011.04.066.

[11] C.K. Colton, Oxygen supply to encapsulated therapeutic cells, Advanced Drug Delivery Reviews 67–68 (2014) 93–110, https://doi.org/10.1016/J.ADDR.2014.02.007.

[12] A.U. Ernst, D.T. Bowers, L.H. Wang, K. Shariati, M.D. Plesser, N.K. Brown, T. Mehrabyan, M. Ma, Nanotechnology in cell replacement therapies for type 1 diabetes, Advanced Drug Delivery Reviews 139 (2019) 116–138, https://doi.org/10.1016/J.ADDR.2019.01.013.

[13] A.U. Ernst, L.H. Wang, M. Ma, Interconnected toroidal hydrogels for islet encapsulation, Advanced Healthcare Materials 8 (12) (2019) 1900423, https://doi.org/10.1002/ADHM.201900423.

[14] M.J. Fowler, Microvascular and Macrovascular complications of diabetes, Clinical Diabetes 29 (3) (2011) 116–122, https://doi.org/10.2337/DIACLIN.29.3.116.

[15] C. Frantz, K.M. Stewart, V.M. Weaver, The extracellular matrix at a glance, Journal of Cell Science 123 (123) (2010) 4195–4200, https://doi.org/10.1242/jcs.023820.

[16] J. Fu, C. Wiraja, H.B. Muhammad, C. Xu, D.A. Wang, Improvement of endothelial progenitor outgrowth cell (EPOC)-mediated vascularization in gelatin-based hydrogels through pore size manipulation, Acta Biomaterialia 58 (2017) 225–237, https://doi.org/10.1016/J.ACTBIO.2017.06.012.

[17] Guimarães, C. F., Gasperini, L., Marques, A. P., & Reis, R. L. (2020). The stiffness of living tissues and its implications for tissue engineering. *Nature Reviews Materials 2020 5:5*, *5*(5), 351–370. doi: 10.1038/s41578-019-0169-1.

[18] M. Haim Zada, A. Kumar, O. Elmalak, E. Markovitz, R. Icekson, A.J. Domb, In vitro and in vivo degradation behavior and the long-term performance of biodegradable PLCL balloon implants, International Journal of Pharmaceutics 574 (2020) 118870, https://doi.org/10.1016/J.IJPHARM.2019.118870.

[19] M. Hasany, A. Thakur, N. Taebnia, F.B. Kadumudi, M.A. Shahbazi, M.K. Pierchala, S. Mohanty, G. Orive, T.L. Andresen, C.B. Foldager, S. Yaghmaei, A. Arpanaei, A. K. Gaharwar, M. Mehrali, A. Dolatshahi-Pirouz, Combinatorial screening of nanoclay-reinforced hydrogels: a glimpse of the "holy grail" in orthopedic stem cell therapy? ACS Applied Materials and Interfaces 10 (41) (2018) 34924–34941, https://doi.org/10.1021/ACSAMI.8B11436/SUPPL_FILE/AM8B11436_SI_001.PDF.

[20] D.I. Holmes, I. Zachary, The vascular endothelial growth factor (VEGF) family: angiogenic factors in health and disease, Genome Biology 6 (2) (2005) 209, https://doi.org/10.1186/gb-2005-6-2-209.

[21] L. Huang, J. Xiang, Y. Cheng, L. Xiao, Q. Wang, Y. Zhang, T. Xu, Q. Chen, H. Xin, X. Wang, Regulation of blood glucose using islets encapsulated in a melanin-modified immune-shielding hydrogel, ACS Applied Materials & Interfaces 13 (11) (2021) 12877–12887, https://doi.org/10.1021/acsami.0c23010.

[22] U. Jammalamadaka, K. Tappa, Recent advances in biomaterials for 3D printing and tissue engineering, Journal of Functional Biomaterials 9 (1) (2018) E22–E, https://doi.org/10.3390/JFB9010022.

[23] D. Janjic, P. Maechler, C. Bartley, A.S. Annen, C.B. Wollheim, Free radical modulation of insulin release in INS-1 cells exposed to alloxan, Biochemical Pharmacology 57 (6) (1999) 639–648, https://doi.org/10.1016/S0006-2952(98)00346-3.

[24] J.-H. Juang, H.-C. Lin, C.-Y. Chen, C.-W. Kao, S.-T. Wu, S.-H. Lin, C.-R. Shen, J.-J. Wang, I.-M. Chu, Subcutaneous transplantation of MIN6 Beta cells embedded in mPEG-ala hydrogel, Diabetes 67 (Supplement_1) (2018), https://doi.org/10.2337/DB18-26-OR.

[25] T. Knobeloch, S.E.M. Abadi, J. Bruns, S. Petrova Zustiak, G. Kwon, Injectable polyethylene glycol hydrogel for islet encapsulation: an *in vitro* and *in vivo* characterization, Biomedical Physics & Engineering Express 3 (3) (2017) 035022, https://doi.org/10.1088/2057-1976/aa742b.

[26] L. Li, G. Zhou, Y. Wang, G. Yang, S. Ding, S. Zhou, Controlled dual delivery of BMP-2 and dexamethasone by nanoparticle-embedded electrospun nanofibers for the efficient repair of critical-sized rat calvarial defect, Biomaterials 37 (2015) 218–229, https://doi.org/10.1016/J.BIOMATERIALS.2014.10.015.

[27] H. Liljebäck, D. Espes, P.-O. Carlsson, Unsurpassed intrahepatic islet engraftment – the quest for new sites for Beta cell replacement, 215517901985766, Cell Medicine 11 (2019), https://doi.org/10.1177/2155179019857662.

[28] J.O. Lim, J.S. Huh, S. Abdi, S.M. Ng, J.J. Yoo, Functionalized biomaterials - oxygen releasing scaffolds, J Biotechnol Biomater 5 (2) (2015) 182, https://doi.org/10.4172/2155-952X.1000182.

[29] C. Liu, Y. Wu, H. Yang, K. Lu, H. Zhang, Y. Wang, J. Wang, L. Ruan, Z. Shen, Q. Yu, Y. Zhang, An injectable alginate/fibrin hydrogel encapsulated with cardiomyocytes and VEGF for myocardial infarction treatment, Journal of Materials Science & Technology 143 (2023) 198–206, https://doi.org/10.1016/J.JMST.2022.11.002.

[30] Liu, Q., Chiu, A., Wang, L. H., An, D., Zhong, M., Smink, A. M., de Haan, B. J., de Vos, P., Keane, K., Vegge, A., Chen, E. Y., Song, W., Liu, W. F., Flanders, J., Rescan, C., Grunnet, L. G., Wang, X., & Ma, M. (2019). Zwitterionically modified alginates mitigate cellular overgrowth for cell encapsulation. *Nature Communications 2019 10:1*, *10*(1), 1–14. doi: 10.1038/s41467-019-13238-7.

[31] Liu, X., Liu, · Song, Feng, S., Wang, X., Bai, W., Xiao, J., Chen, · Dongliang, Xiong, C., & Zhang, L. (2021). Thermal, mechanical and degradation properties of flexible poly (1,3-trimethylene carbonate)/poly (L-lactide-co-ε-caprolactone) blends. *Journal of Polymer Research*, *1*, 3. doi: 10.1007/s10965-021-02802-9.

[32] Liu, X., Yu, Y., Liu, D., Li, J., Sun, J., Wei, Q., Zhao, Y., Pandol, S. J., & Li, L. (2022). Porous microcapsules encapsulating β cells generated by microfluidic electrospray technology for diabetes treatment. *NPG Asia Materials 2022 14:1*, *14*(1), 1–10. doi: 10.1038/s41427-022-00385-5.

[33] Y. Lu, J. Huang, G. Yu, R. Cardenas, S. Wei, E.K. Wujcik, Z. Guo, Coaxial electrospun fibers: applications in drug delivery and tissue engineering, Wiley

Interdisciplinary Reviews: Nanomedicine and Nanobiotechnology 8 (5) (2016) 654–677, https://doi.org/10.1002/WNAN.1391.
[34] A. Luraghi, F. Peri, L. Moroni, Electrospinning for drug delivery applications: a review, Journal of Controlled Release 334 (2021) 463–484, https://doi.org/10.1016/J.JCONREL.2021.03.033.
[35] A. Merglen, S. Theander, B. Rubi, G. Chaffard, C.B. Wollheim, P. Maechler, Glucose sensitivity and metabolism-secretion coupling studied during two-Year continuous culture in INS-1E insulinoma cells, Endocrinology 145 (2) (2004) 667–678, https://doi.org/10.1210/EN.2003-1099.
[36] M. Padmasekar, N. Lingwal, B. Samikannu, C. Chen, H. Sauer, T. Linn, Exendin-4 protects hypoxic islets from oxidative stress and improves islet transplantation outcome, Endocrinology 154 (4) (2013) 1424–1433, https://doi.org/10.1210/EN.2012-1983.
[37] S. Pellegrini, Alternative transplantation sites for islet transplantation, Transplantation, Bioengineering, and Regeneration of the Endocrine Pancreas: 1 (2020) 833–847, https://doi.org/10.1016/B978-0-12-814833-4.00065-4.
[38] K.C. Scheiner, R.F. Maas-Bakker, T.T. Nguyen, A.M. Duarte, G. Hendriks, L. Sequeira, G.P. Duffy, R. Steendam, W.E. Hennink, R.J. Kok, Sustained release of Vascular endothelial growth factor from poly(ε-caprolactone-PEG-ε-caprolactone)-b-poly(l-lactide) multiblock Copolymer microspheres, ACS Omega 4 (7) (2019) 11481–11492, https://doi.org/10.1021/ACSOMEGA.9B01272.
[39] A.M.J. Shapiro, M. Pokrywczynska, C. Ricordi, Clinical pancreatic islet transplantation, Nature Reviews. Endocrinology 13 (5) (2017) 268–277, https://doi.org/10.1038/NRENDO.2016.178.
[40] E.A. Silva, D.J. Mooney, Effects of VEGF temporal and spatial presentation on angiogenesis, Biomaterials 31 (6) (2010) 1235–1241, https://doi.org/10.1016/J.BIOMATERIALS.2009.10.052.
[41] Y. Su, M.S. Toftdal, A.L. Friec, M. Dong, X. Han, M. Chen, 3D electrospun synthetic Extracellular matrix for tissue regeneration, Small Science 1 (7) (2021) 2100003, https://doi.org/10.1002/SMSC.202100003.
[42] M.S. Toftdal, N. Taebnia, F.B. Kadumudi, T.L. Andresen, T. Frogne, L. Winkel, L. G. Grunnet, A. Dolatshahi-Pirouz, Oxygen releasing hydrogels for beta cell assisted therapy, International Journal of Pharmaceutics 602 (2021) 120595, https://doi.org/10.1016/J.IJPHARM.2021.120595.
[43] P. Vempati, A.S. Popel, F. Mac Gabhann, Extracellular regulation of VEGF: isoforms, proteolysis, and vascular patterning, Cytokine & Growth Factor Reviews 25 (1) (2014) 1–19, https://doi.org/10.1016/j.cytogfr.2013.11.002.
[44] L.H. Wang, A.U. Ernst, J.A. Flanders, W. Liu, X. Wang, A.K. Datta, B. Epel, M. Kotecha, K.K. Papas, M. Ma, An inverse-breathing encapsulation system for cell delivery. *science*, Advances 7 (20) (2021), https://doi.org/10.1126/SCIADV.ABD5835/SUPPL_FILE/ABD5835_SM.PDF.
[45] X. Wang, K.G. Maxwell, K. Wang, D.T. Bowers, J.A. Flanders, W. Liu, L.H. Wang, Q. Liu, C. Liu, A. Naji, Y. Wang, B. Wang, J. Chen, A.U. Ernst, J.M. Melero-Martin, J.R. Millman, M. Ma, A nanofibrous encapsulation device for safe delivery of insulin-producing cells to treat type 1 diabetes, Science Translational Medicine 13 (596) (2021), https://doi.org/10.1126/SCITRANSLMED.ABB4601.
[46] Wang, Y., Yokota, T., & Someya, T. (2021). Electrospun nanofiber-based soft electronics. *NPG Asia Materials 2021 13:1*, *13*(1), 1–22. doi: 10.1038/s41427-020-00267-8.
[47] J.D. Weaver, D.M. Headen, J. Aquart, C.T. Johnson, L.D. Shea, H. Shirwan, A. J. García, Vasculogenic hydrogel enhances islet survival, engraftment, and function in leading extrahepatic sites. *science*, Advances 3 (6) (2017), https://doi.org/10.1126/SCIADV.1700184/SUPPL_FILE/1700184_SM.PDF.
[48] C.A. Welsch, W.L. Rust, M. Csete, Concise review: lessons Learned from islet transplant clinical trials in developing stem cell therapies for type 1 diabetes, Stem Cells Translational Medicine 8 (3) (2019) 209–214, https://doi.org/10.1002/SCTM.18-0156.
[49] World Health Organization. (2016). *Global Report on Diabetes*.
[50] R. Xu, Z. Zhang, M.S. Toftdal, A.C. Møller, F. Dagnaes-Hansen, M. Dong, J. S. Thomsen, A. Brüel, M. Chen, Synchronous delivery of hydroxyapatite and connective tissue growth factor derived osteoinductive peptide enhanced osteogenesis, Journal of Controlled Release : Official Journal of the Controlled Release Society 301 (2019) 129–139, https://doi.org/10.1016/J.JCONREL.2019.02.037.
[51] N. Yin, Y. Han, H. Xu, Y. Gao, T. Yi, J. Yao, L. Dong, D. Cheng, Z. Chen, VEGF-conjugated alginate hydrogel prompt angiogenesis and improve pancreatic islet engraftment and function in type 1 diabetes, Materials Science and Engineering: C 59 (2016) 958–964, https://doi.org/10.1016/j.msec.2015.11.009.
[52] N. Zhang, A. Richter, J. Suriawinata, S. Harbaran, J. Altomonte, L. Cong, H. Zhang, K. Song, M. Meseck, J. Bromberg, H. Dong, Elevated vascular endothelial growth factor production in islets improves islet graft vascularization, Diabetes 53 (4) (2004) 963–970, https://doi.org/10.2337/DIABETES.53.4.963.
[53] X. Zhang, J. Li, P. Ye, G. Gao, K. Hubbell, X. Cui, Coculture of mesenchymal stem cells and endothelial cells enhances host tissue integration and epidermis maturation through AKT activation in gelatin methacryloyl hydrogel-based skin model, Acta Biomaterialia 59 (2017) 317–326, https://doi.org/10.1016/j.actbio.2017.07.001.
[54] X. Zhang, K. Wang, J. Hu, Y. Zhang, Y. Dai, F. Xia, Role of a high calcium ion content in extending the properties of alginate dual-crosslinked hydrogels, Journal of Materials Chemistry A 8 (47) (2020) 25390–25401, https://doi.org/10.1039/D0TA09315G.